

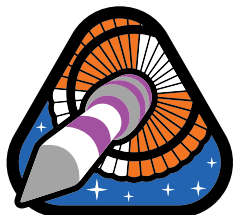
Modeling and Flight Performance of Supersonic Disk-Gap-Band Parachutes in Slender Body Wakes

Suman Muppidi

AMA Inc., NASA Ames Research Center

Clara O'Farrell, Christopher Tanner, Ian Clark

Jet Propulsion Laboratory, California Institute of Technology

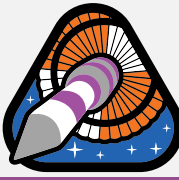


ASPIRE

AIAA Atmospheric Flight Mechanics Conference, Atlanta, GA, June 27th 2018

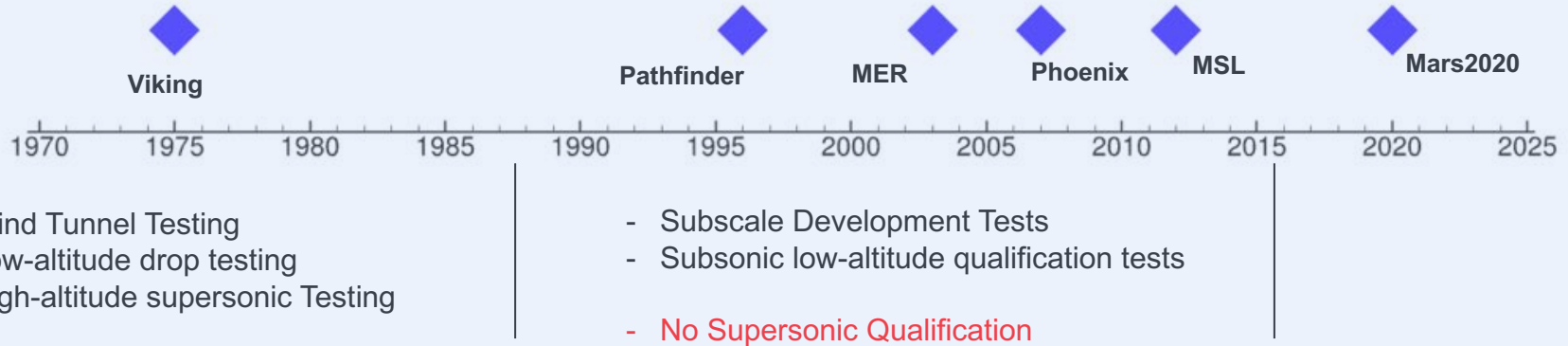


Introduction



ASPIRE

- Disk-Gap-Band (DGB) parachutes have been used on all US Mars missions.
- All of the parachutes have been variants of the Viking DGB parachute.

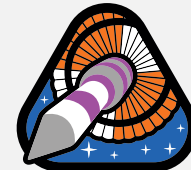


- Since Viking era,
 - Parachute materials have changed (Dacron → Kevlar, Nylon)
 - Analysis methods have become smarter
 - Parachute size and load have increased
 - Design Margins have decreased
- Relationship between flight performance and subsonic testing is not clear

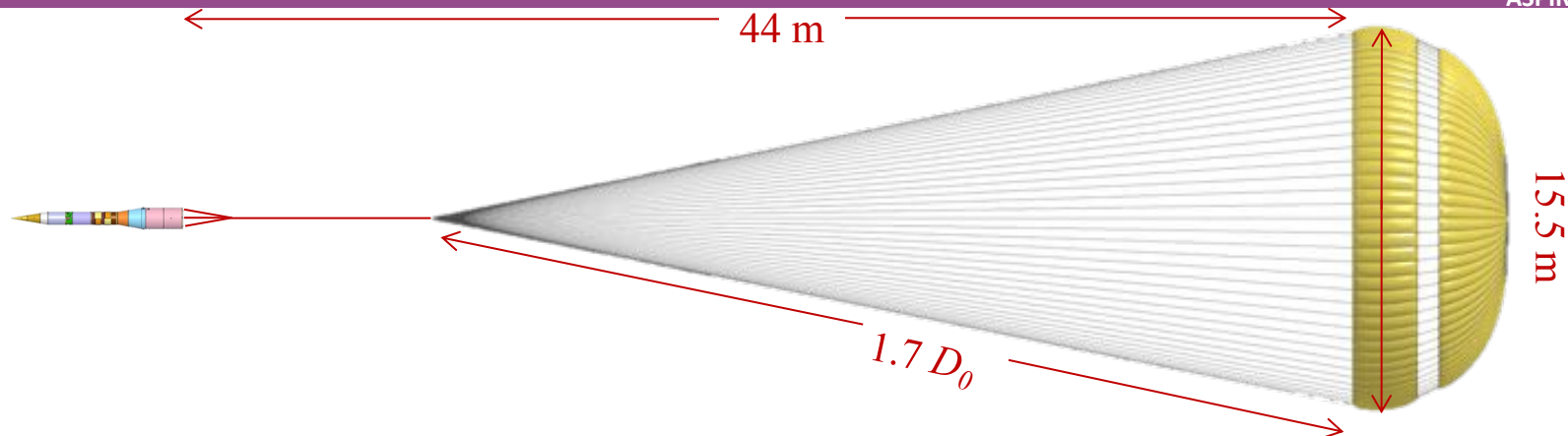


The Advanced Supersonic Parachute Inflation Research and Experiments (ASPIRE) project is tasked with deployment and testing of full-scale *Disk-Gap-Band* parachutes at Mars relevant conditions

ASPIRE



ASPIRE



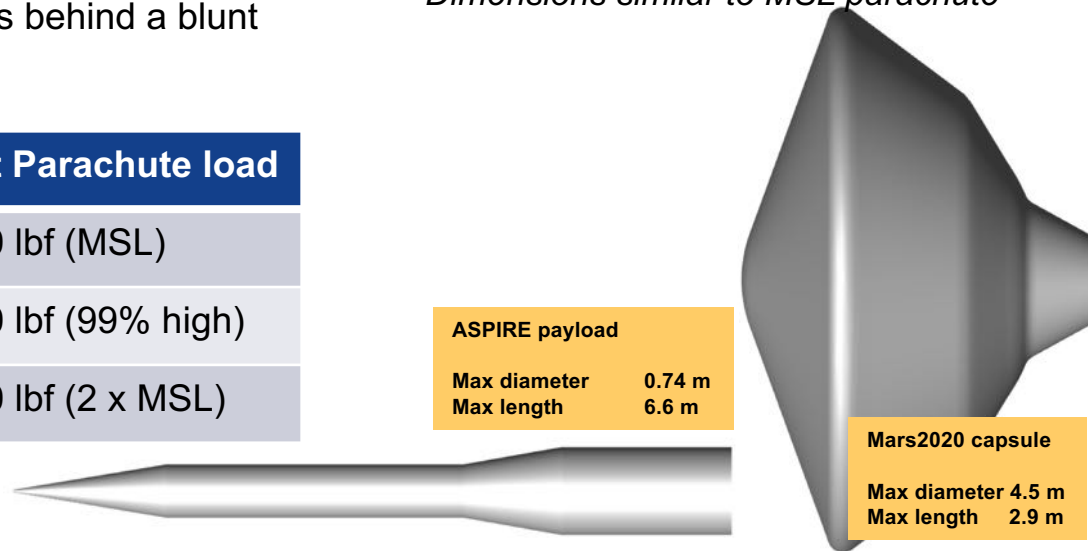
- Parachutes are deployed in the wake of a slender body (at high altitudes over Earth).
- Two different parachutes are being tested.
- The qualified parachute will be used at Mars behind a blunt body (*Mars2020*).

ASPIRE Disk-Gap-Band (DGB) Parachute

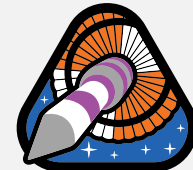
- Reference Diameter (D_0) 21.5 m
- Inflated Diameter 15.5 m

Dimensions similar to MSL parachute

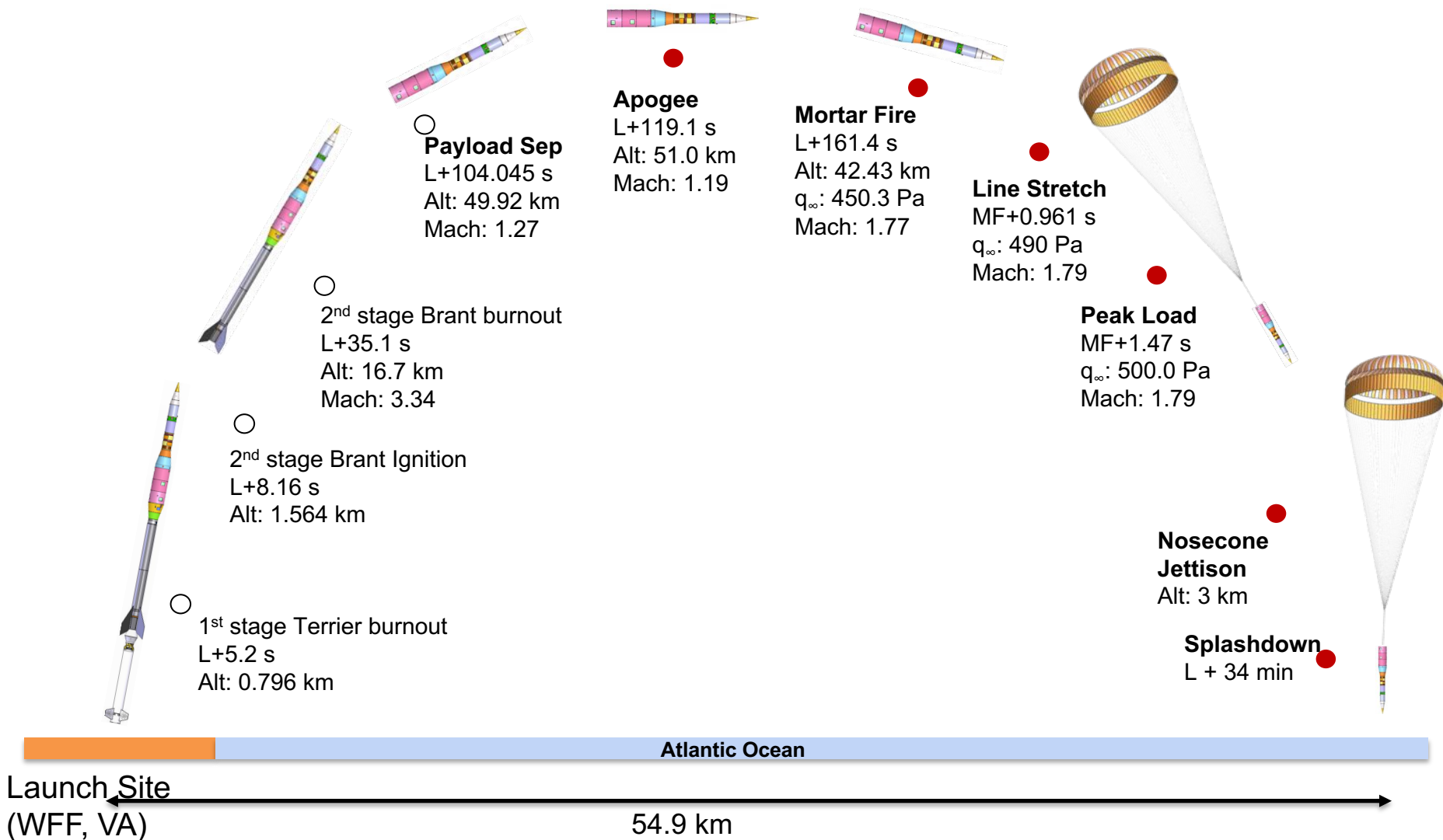
| Test | Parachute | Target Parachute load |
|-----------------|--------------------|-----------------------|
| SR01 (Oct 2017) | MSL built-to-print | 35 000 lbf (MSL) |
| SR02 (Mar 2018) | Strengthened | 47 000 lbf (99% high) |
| SR03 (Jul 2018) | Strengthened | 70 000 lbf (2 x MSL) |



ASPIRE Flight Test

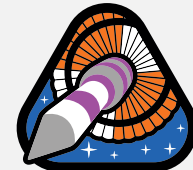


ASPIRE

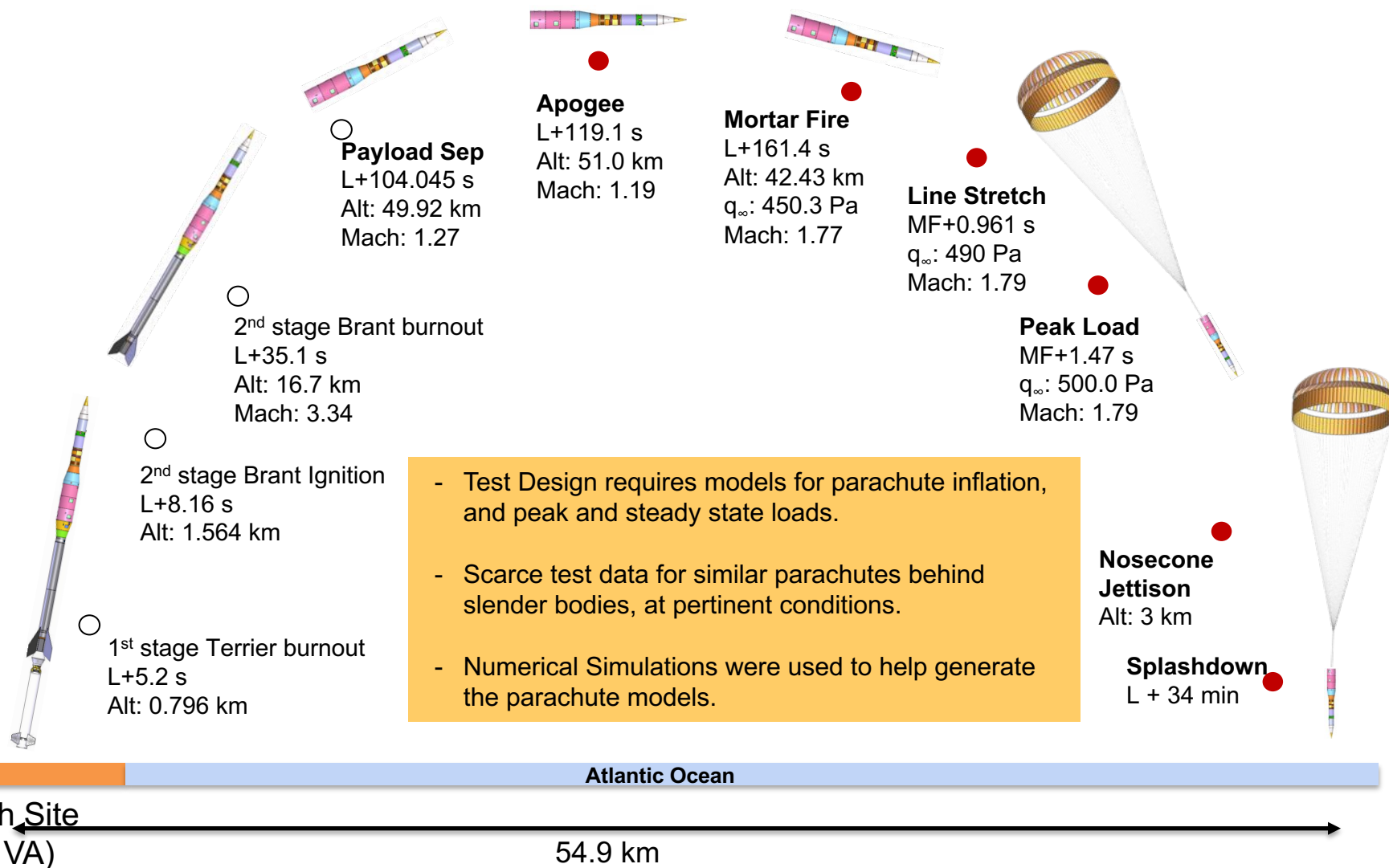


Note: The numbers indicate actual quantities from first flight test (SR01), Oct 2017.

ASPIRE Flight Test



ASPIRE



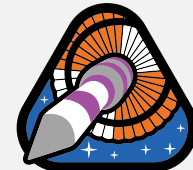
- Test Design requires models for parachute inflation, and peak and steady state loads.

- Scarce test data for similar parachutes behind slender bodies, at pertinent conditions.

- Numerical Simulations were used to help generate the parachute models.

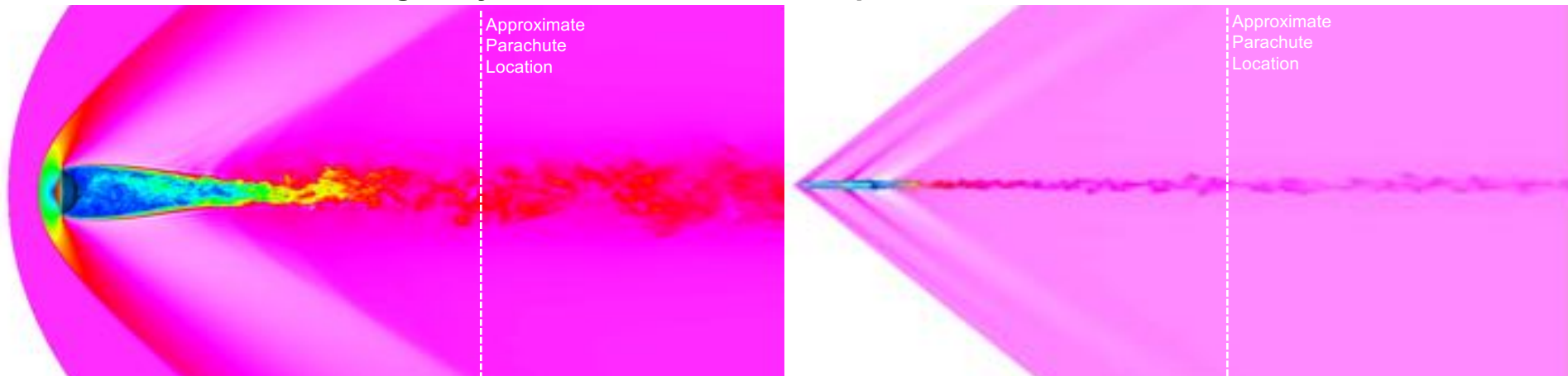
Note: The numbers indicate actual quantities from first flight test (SR01), Oct 2017.

Wake Simulations



ASPIRE

- Q. How does the leading body affect the mean and temporal wake characteristics ?



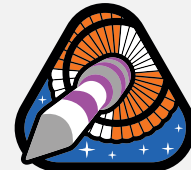
Freestream Details

| Atmosphere | Density/Altitude | Velocity | Mach Number | Dynamic Pressure |
|------------------|---|-----------|-------------|------------------|
| Air, perfect gas | 0.00346 (Kg/m ³)/ 41 km over Earth | 558.2 m/s | 1.75 | 538 Pa |

Challenges:

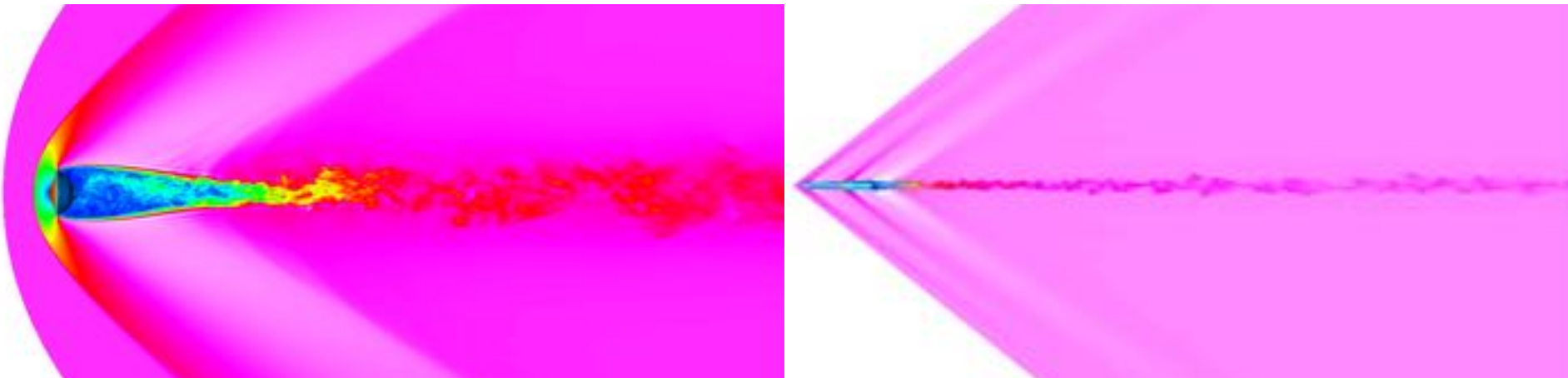
1. Wakes are highly unsteady and turbulent.
2. The region of interest (40-50m downstream of the leading body) demands large computational domains
3. Unstructured meshes make the combination of large domains and adequate resolution manageable
4. Dissipative numerics and solvers are ill-suited

Wake Simulations



ASPIRE

- Q. How does the leading body affect the mean and temporal wake characteristics ?



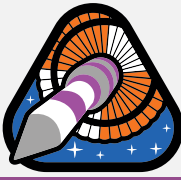
Freestream Details

| Atmosphere | Density/Altitude | Velocity | Mach Number | Dynamic Pressure |
|------------------|---|-----------|-------------|------------------|
| Air, perfect gas | 0.00346 (Kg/m ³)/ 41 km over Earth | 558.2 m/s | 1.75 | 538 Pa |

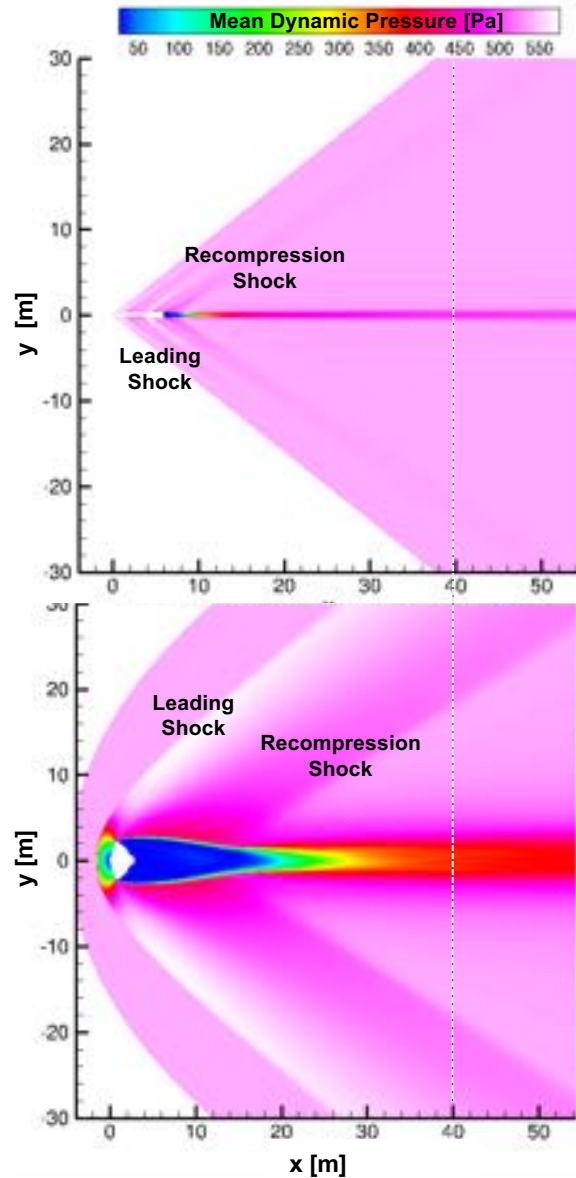
Numerical Details

1. Simulations are performed using US3D, a flow simulation software developed by UMN and NASA.
2. DES97 simulations using Spalart-Almaras one-equation turbulence model
3. Flux computation using US3D's low-numerical-dissipation schemes (2nd order fluxes).
4. Time advancement using Implicit Euler (2nd order, point-relaxation).
5. Unstructured computational meshes contain tetrahedral, prism and hexahedral cells.

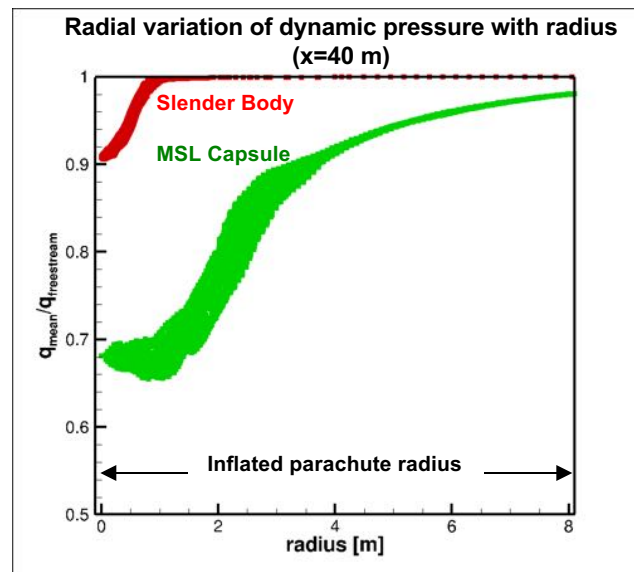
Mean Flow Field



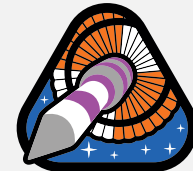
ASPIRE



- In general, wake characteristics scale with the diameter; $D_{\text{MSL}}/D_{\text{ASPIRE}} \sim 6$
- The wake behind the slender body closes much earlier; is thinner.
- Dynamic pressure recovery (q_{min}) much faster behind the slender body, compared to the blunt body.
- Deficit (velocity, dynamic pressure) is larger, behind the blunt body.
- Parachute drag is directly dependent on dynamic pressure. We should expect lower drag behind a blunt body.

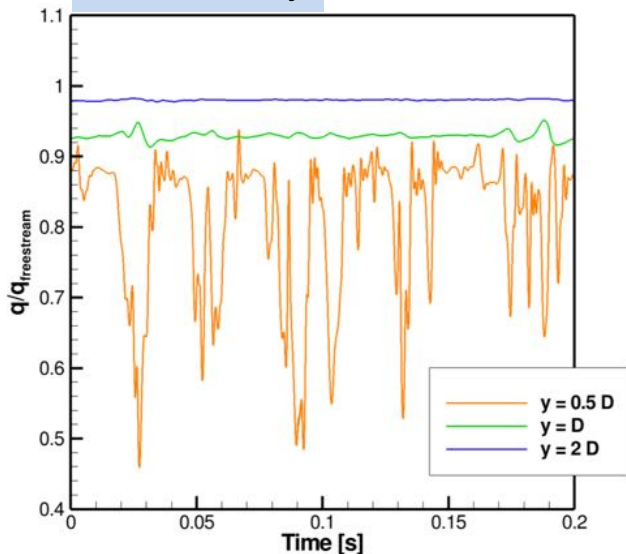


Temporal Unsteadiness

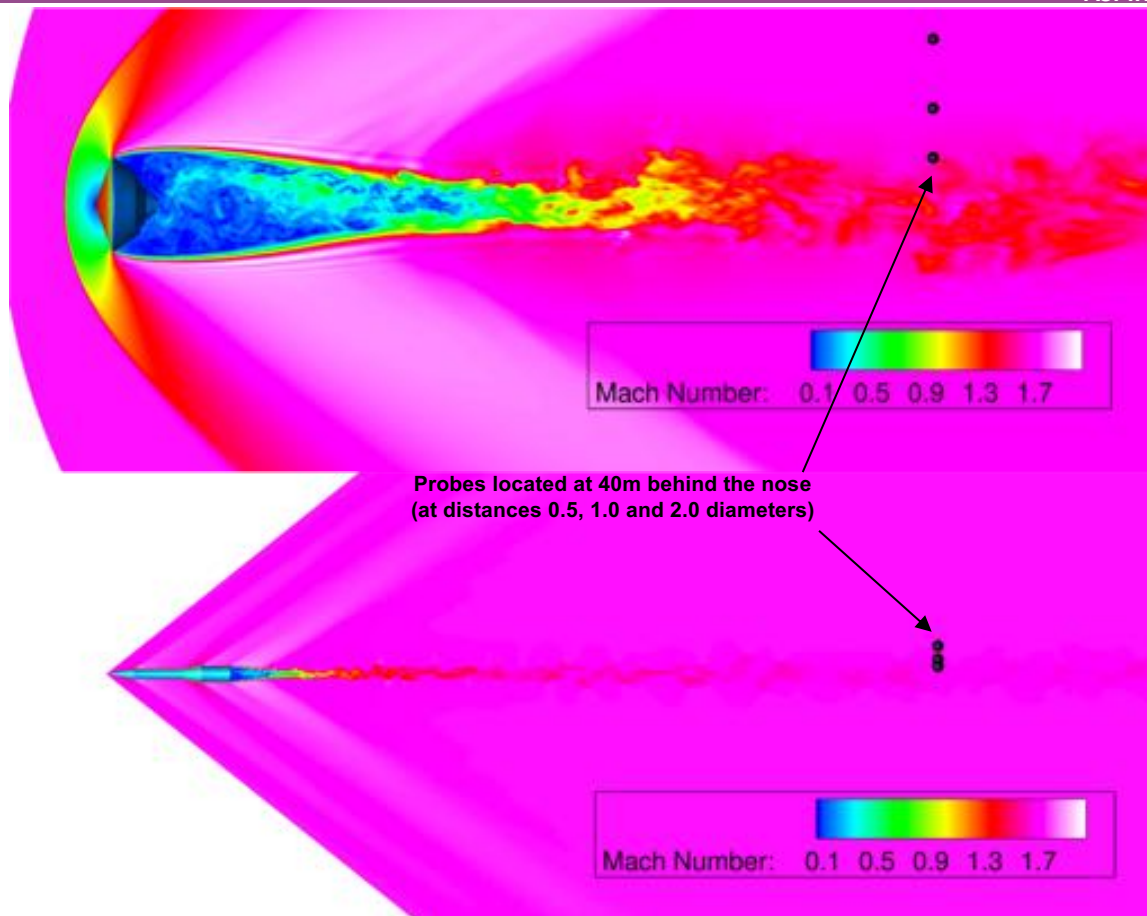
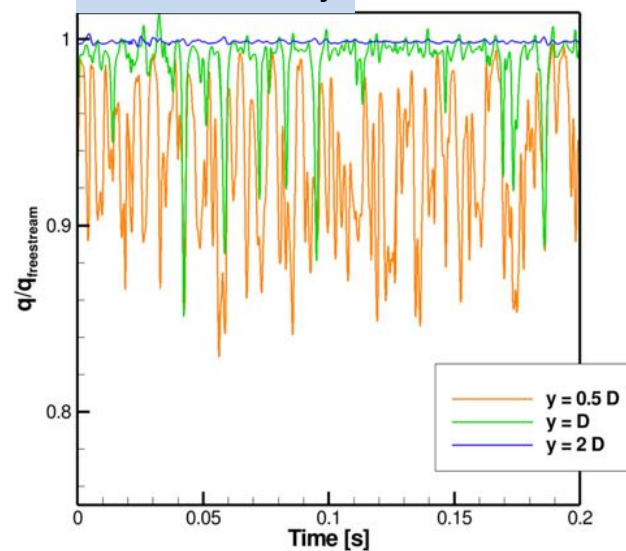


ASPIRE

Behind blunt body



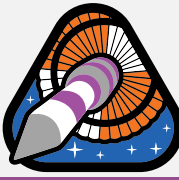
Behind slender body



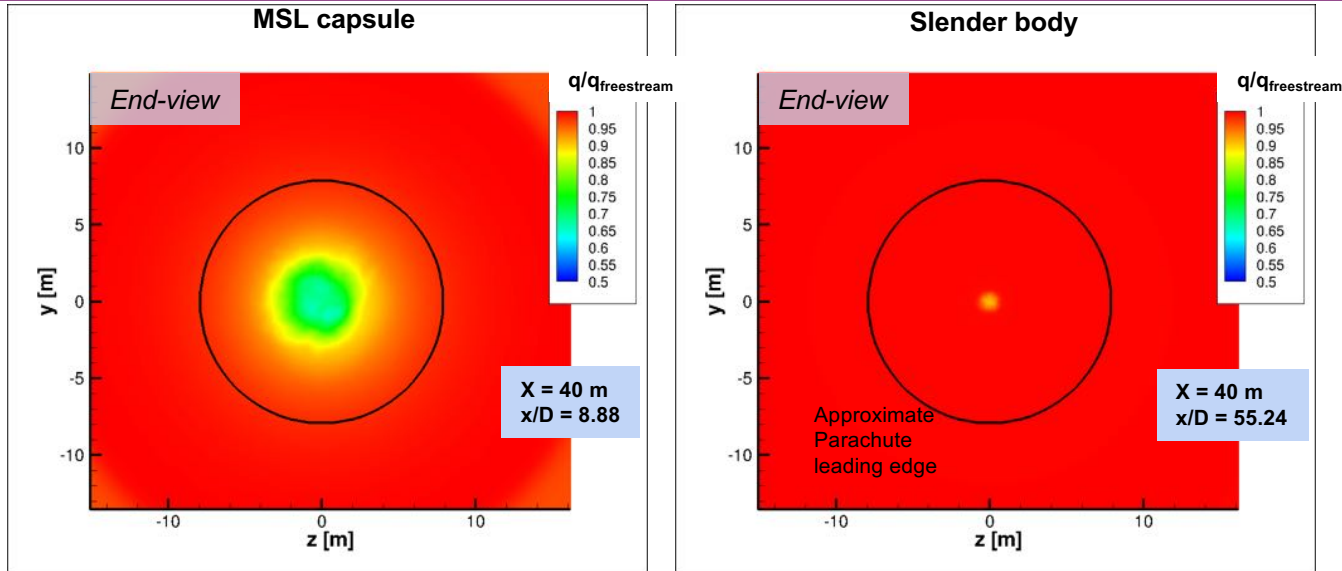
Probes located at 40m behind the nose
(at distances 0.5, 1.0 and 2.0 diameters)

- Outside the wake (roughly diameter of the leading body), the flow is fairly steady
- The frequency of unsteadiness is higher behind the slender body.
- Larger peak-to-peak variation behind the blunt body.

Implications to Flight Test Design



ASPIRE



- Parachute pack behind a blunt body could see a dynamic pressure 50-90% of freestream value; this likely range is smaller behind a slender body: 90-100% of freestream dynamic pressure.

- *Parachute inflation behind a slender body could be more stressing.*

- Peak parachute load (M2020 model) is estimated as a function of the freestream dynamic pressure as

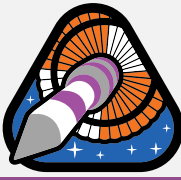
$$F_{peak} = k_p(2q_{\infty}S_p)$$

S_p : Parachute Projected Area
 q_{∞} : Freestream Dynamic Pressure
 k_p : Inflation constant

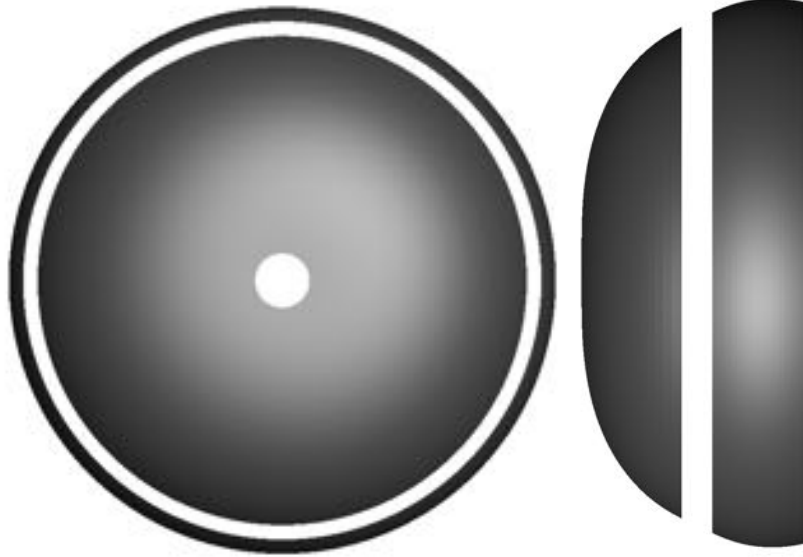
- For MSL/M2020 parachute, estimated range of k_p is 0.76 to 0.90.

- ASPIRE payload has a smaller wake deficit → adjusted k_p range: 0.76 to 0.98.
 (for the same dynamic pressure and parachute, higher inflation load behind the ASPIRE payload)

Simplified Parachute Simulations

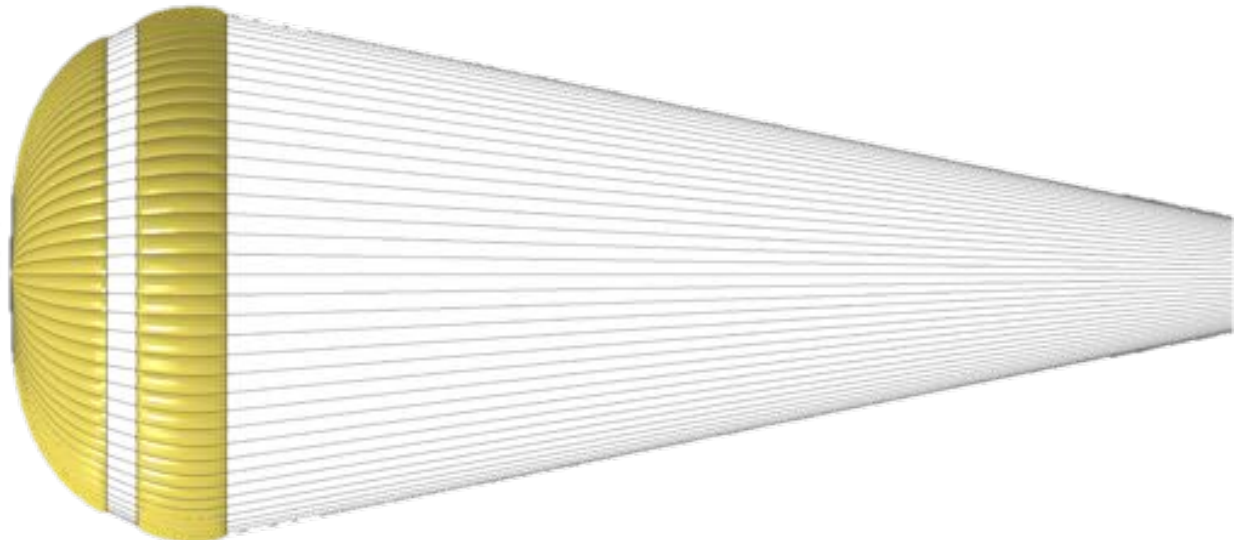


ASPIRE

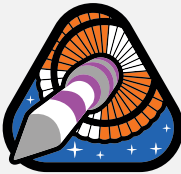


- Parachute simplified as a surface of revolution.
- Treated as rigid, impermeable, 1mm shell.
- Risers and lines are not modeled.
- Geometry maintains the disk-gap-band configuration.
- Parachute is placed 45 m behind the leading body.
- Same freestream as the wake simulations
 - Mach number 1.75; Dynamic Pressure 538 Pa

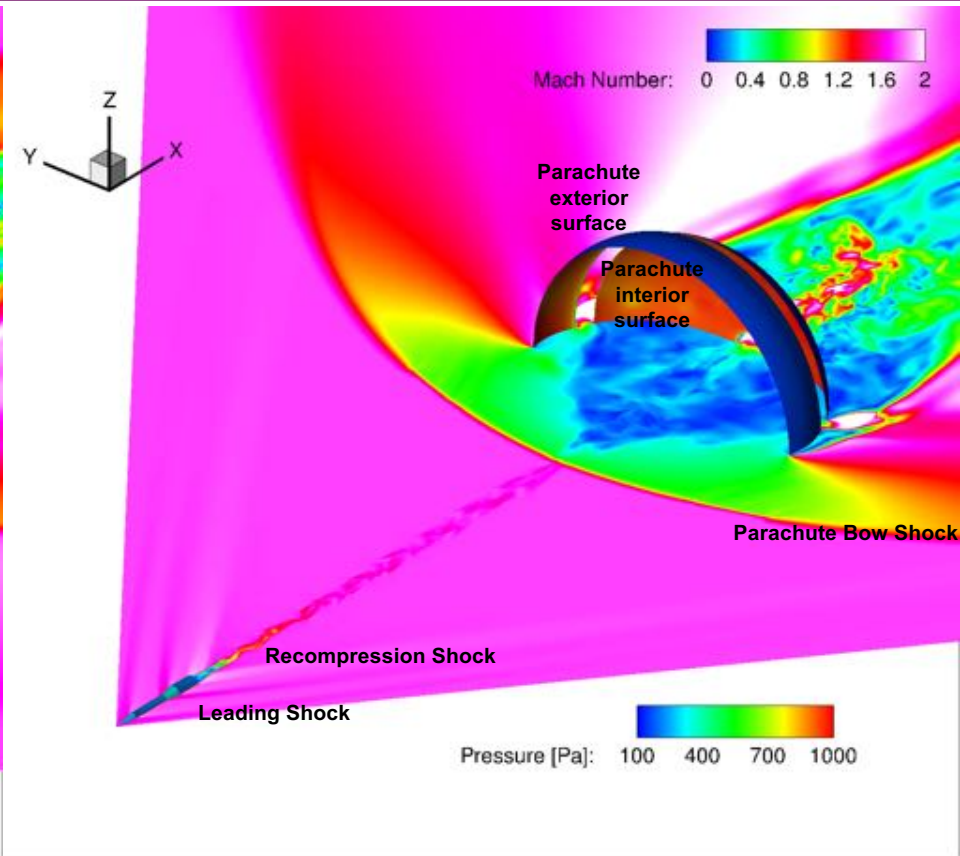
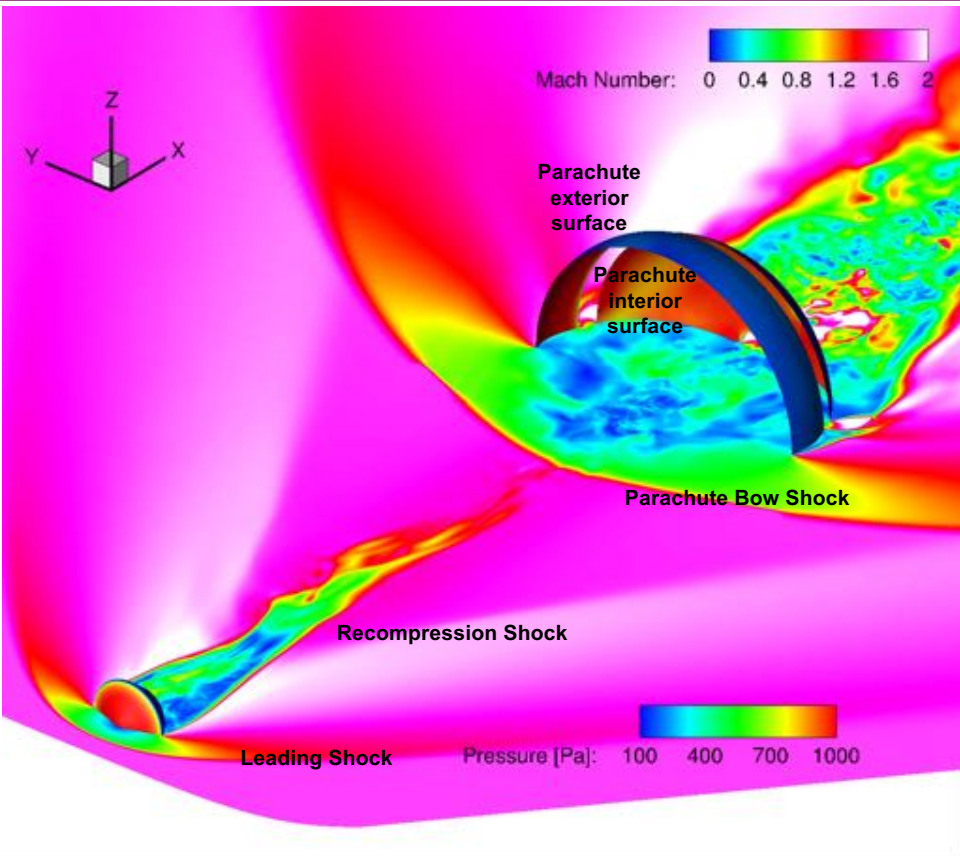
Q. What is the effect of the leading body on the steady-state parachute drag ?



Effect of Leading Body

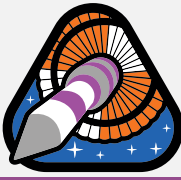


ASPIRE

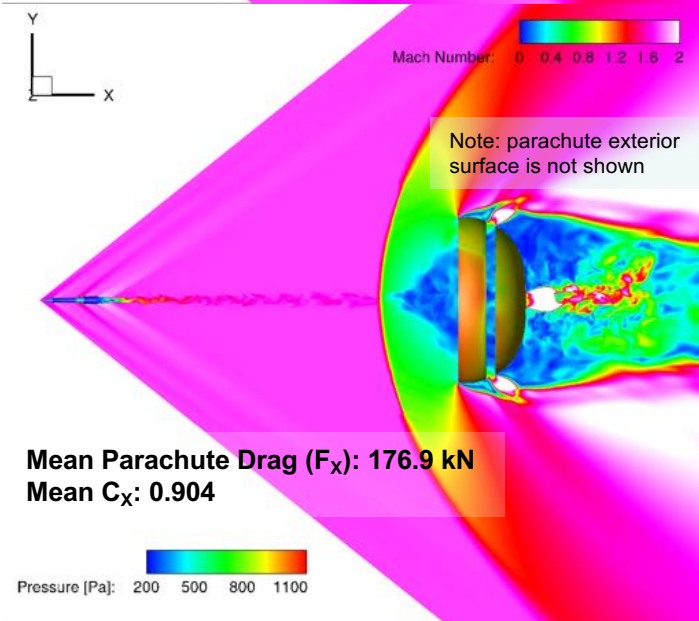
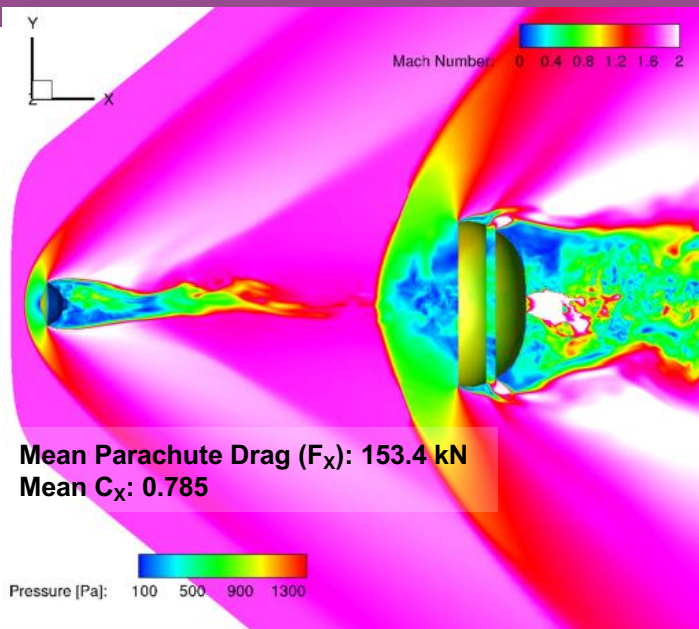


- Unsteady flow starting at the wake of the leading body; flow acceleration through the vent and the gap.
- Interaction between the wake and the parachute shock is more apparent behind the blunt body.
- Behind the slender body, the parachute bow shock barely registers the (narrow) wake.

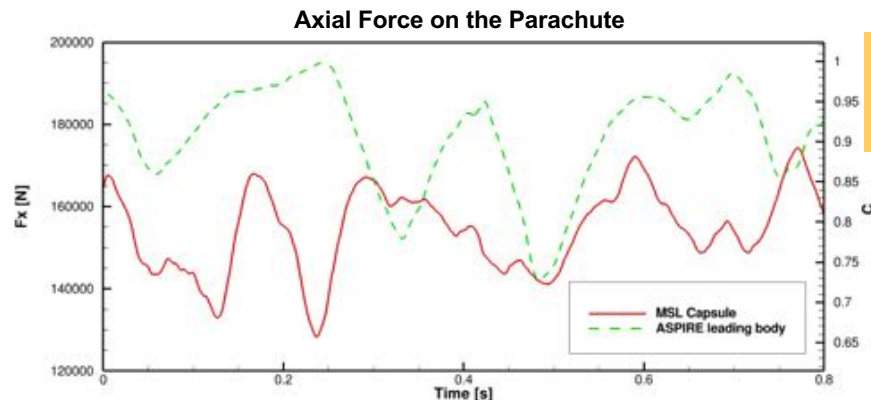
Effect of Leading Body



ASPIRE



- Qualitatively, interaction between the leading body and the parachute appears stronger for the blunt body.
- Even for a rigid geometry, Parachute drag is unsteady.
- Mean parachute drag behind the slender body is about 15 % higher (than that on the blunt body).
- This difference is consistent with the larger wake deficit behind the blunt body.
- Also consistent with wind tunnel data from past studies (Reichenau *et al.* 1972 report 6-12% increase at Mach 1.0-1.4)



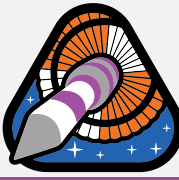
Compare to leading body drag:

Slender Body : 69 N
MSL Capsule : 12 800 N

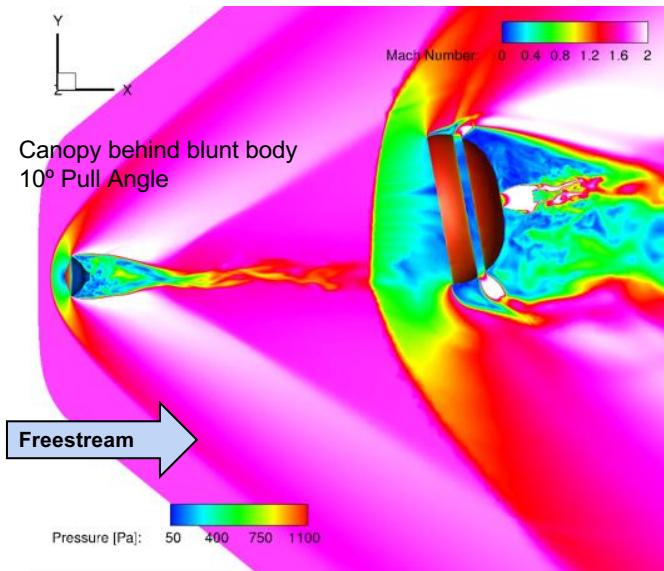
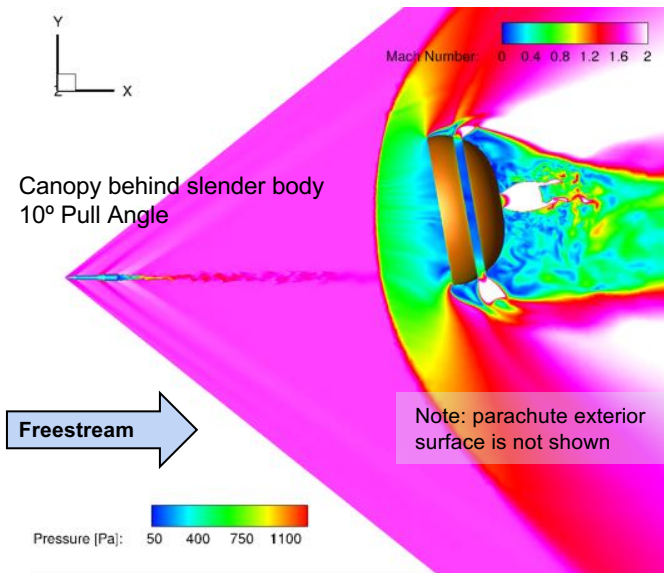
$$C_x = F_x / (\text{freestream dynamic pressure} * \text{parachute reference area})$$

[Parachute reference diameter = 21.5 m]

Effect of Pull Angle

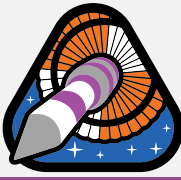


ASPIRE



- Parachutes are rarely along the axis; exhibit a preferential off-axis orientation.
- Current simulations placed the parachute at pull angles of 5° and 10° (behind both the slender and the blunt bodies); freestream is aligned with the leading body axis.
- The parachutes were rotated about the nose of the leading body.
- With these configurations, grid generation is an challenge (we lose an axis of revolution).
- As with 0° pull angle, the forces on the Parachute, and the flow past the parachute, are unsteady.
- *Q. How does the parachute force vary with pull angle ?*

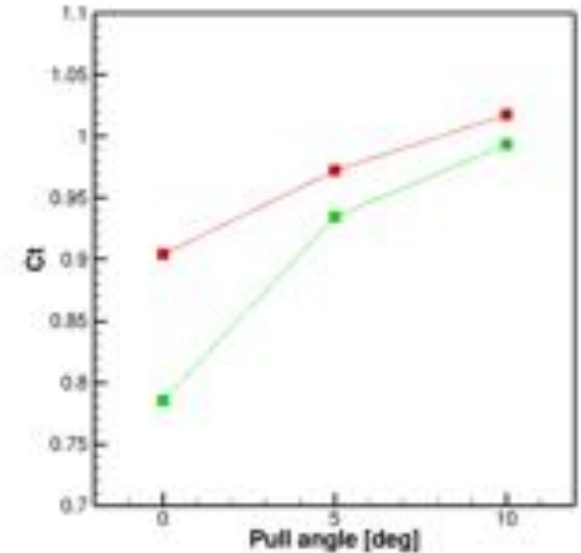
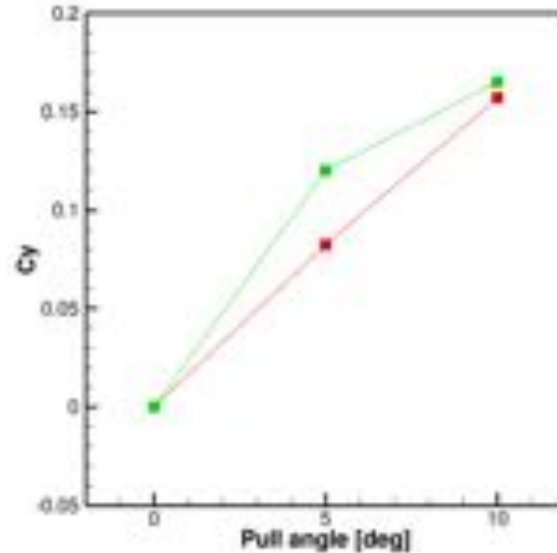
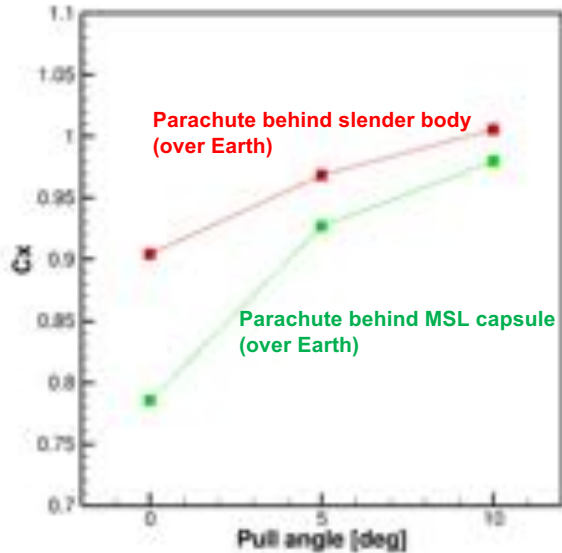
Canopy Drag Comparison



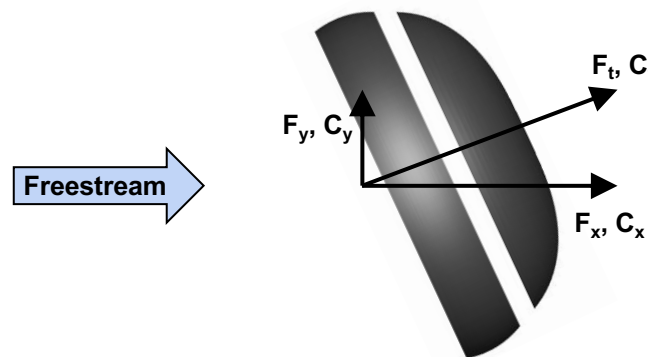
ASPIRE

$C_{x,y} = F_{x,y} / (\text{freestream dynamic pressure} * \text{canopy reference area})$
 Canopy reference diameter = 21.5 m; Reference area = 363.04 m²

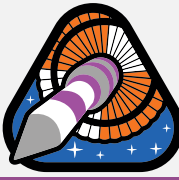
$$C_t = (C_x^2 + C_y^2)^{1/2}$$



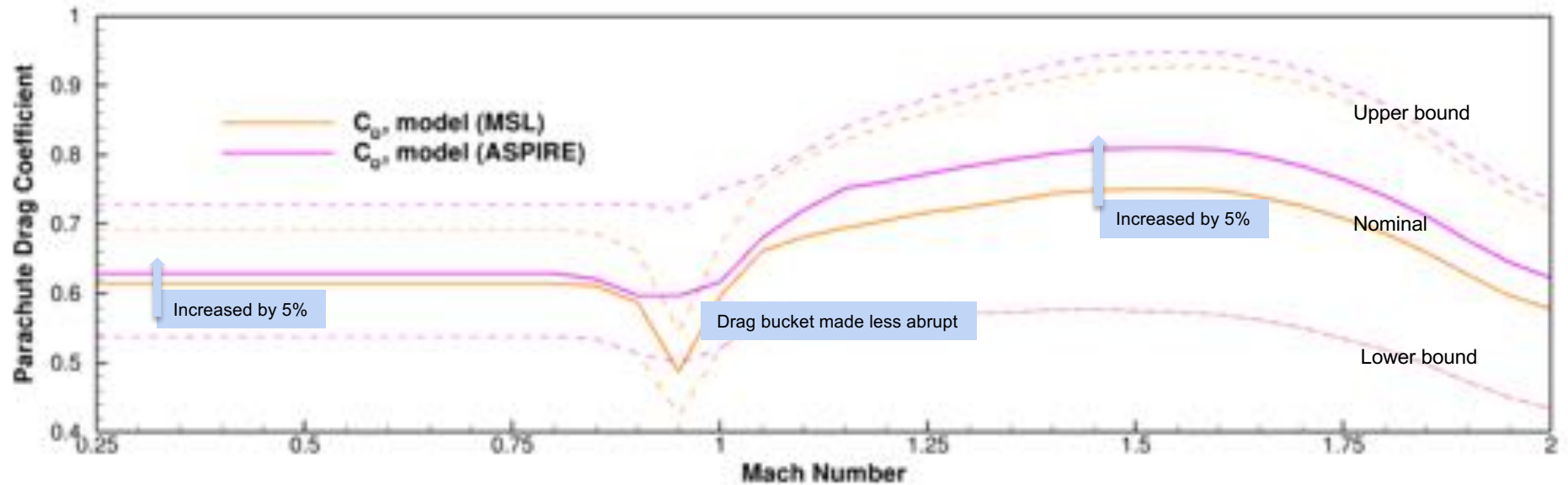
With increasing pull angle, the canopy moves out of the wake and the drag discrepancy decreases.



Development of Pre-Flight Drag Model

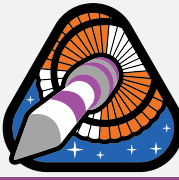


ASPIRE



- MSL parachute drag model was modified to yield the ASPIRE parachute drag model.
- The modifications were informed by flight and wind tunnel tests, and numerical simulations
 - Subsonic: Increased nominal drag performance and the high margin; retained the low margin
 - Supersonic: Increased nominal drag performance and the high margin; retained the low margin
 - Transonic: reduced the steep reduction at near-sonic conditions; blended the subsonic and supersonic drag curves
- The ASPIRE drag model (and the bounds) was used in the flight mechanics simulations, and to help design the flight tests.

Air vs CO₂

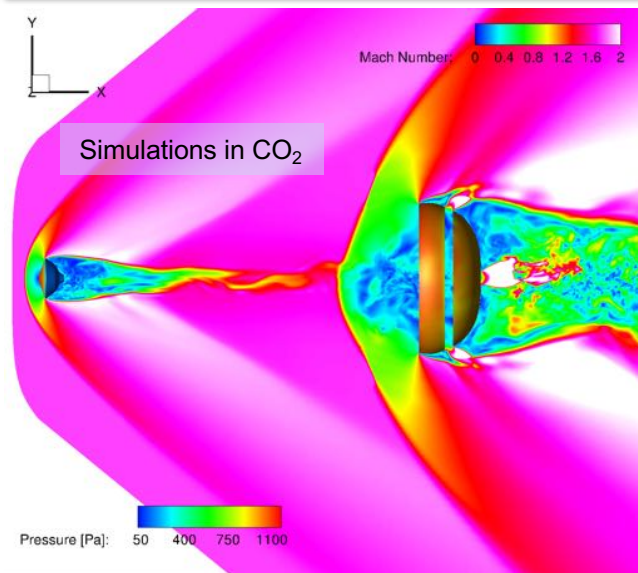


ASPIRE

Q. What is the effect of the freestream gas on the parachute drag ?

Freestream Details

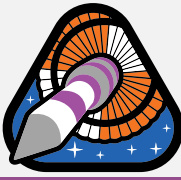
| Atmosphere | Density/Altitude | Velocity | Mach Number | Dynamic Pressure |
|-------------------------------|------------------------------|-----------|-------------|------------------|
| Air, perfect gas | 0.00346 (Kg/m ³) | 558.2 m/s | 1.75 | 538 Pa |
| CO ₂ , perfect gas | 0.00605 (Kg/m ³) | 421.8 m/s | 1.75 | 538 Pa |



- Simulations of parachute behind the MSL capsule in air and CO₂ at the *same Mach number and freestream dynamic pressure*.
- The two fluids have different values for ratio of Specific Heats (γ):
 - Air: 1.4
 - CO₂: 1.3
- γ affects shock standoff distance and conditions across the shock, which in turn affect pressure on the parachute, and the parachute performance.
- Simulations at M 1.75 show very similar performance in both gases (unsteadiness, and parachute drag); mean parachute drag varies by only 2%.
- γ -effects not very significant at this Mach number (e.g. post-shock total pressure ratio is within 2.5%).

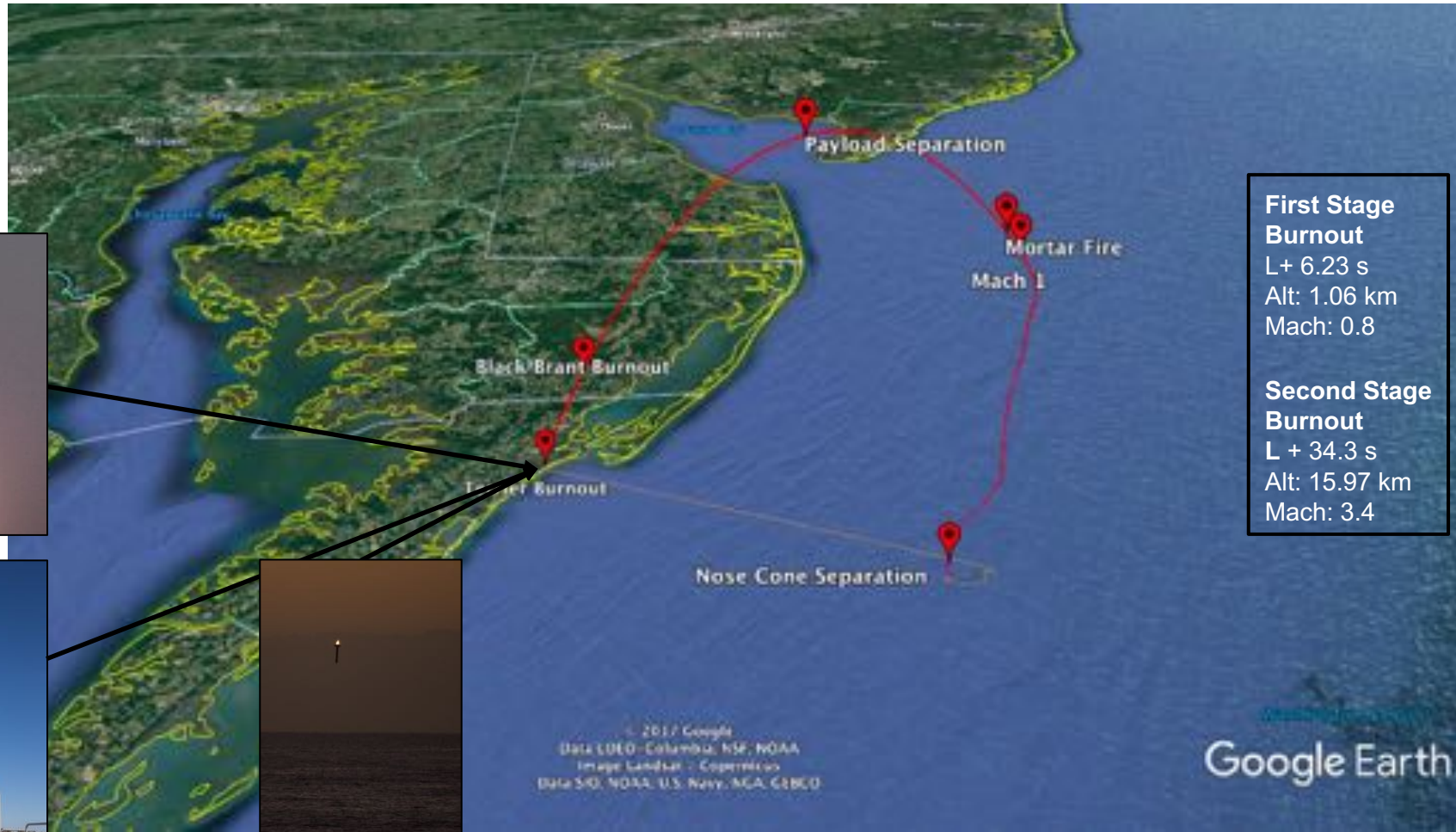
Simulations indicate that at this Mach number, a high-altitude Earth test is a good proxy for a Mars flight

SR01 Flight Test



ASPIRE

The First Few seconds



First Stage Burnout

L+ 6.23 s
Alt: 1.06 km
Mach: 0.8

Second Stage Burnout

L + 34.3 s
Alt: 15.97 km
Mach: 3.4

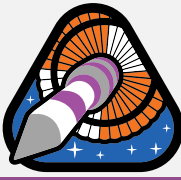


Launch 6:45 EDT.
Wallops Island, VA

1st stage burnout
L+6.2 s (1 km)

4th October, 2017

SR01 Flight Test



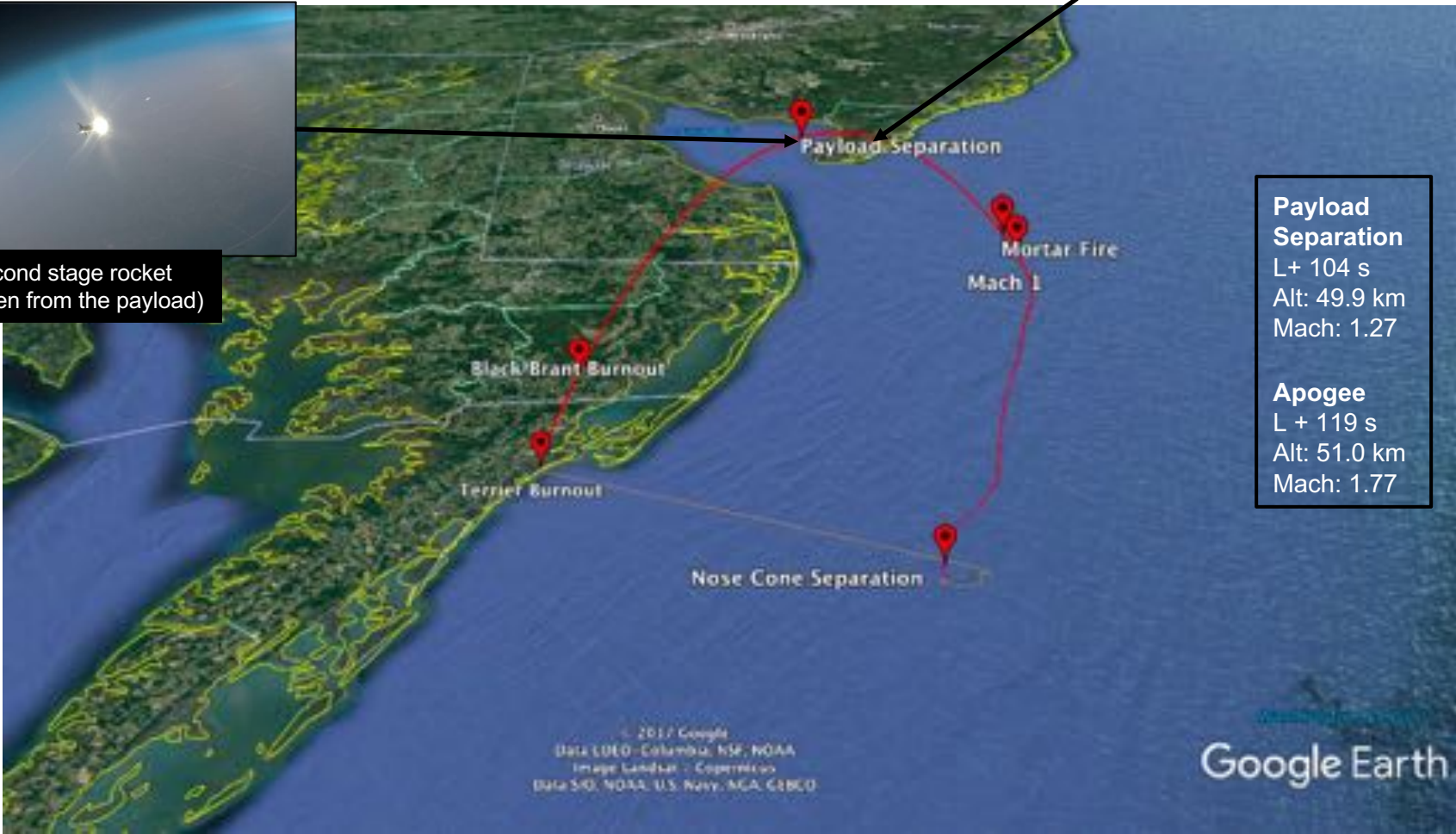
ASPIRE

High Above the Earth

Apogee
L+119 s (51 km)



Second stage rocket
(as seen from the payload)

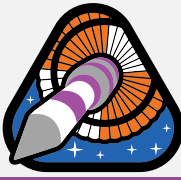


Payload Separation
L+ 104 s
Alt: 49.9 km
Mach: 1.27

Apogee
L + 119 s
Alt: 51.0 km
Mach: 1.77

Google Earth

SR01 Flight Test

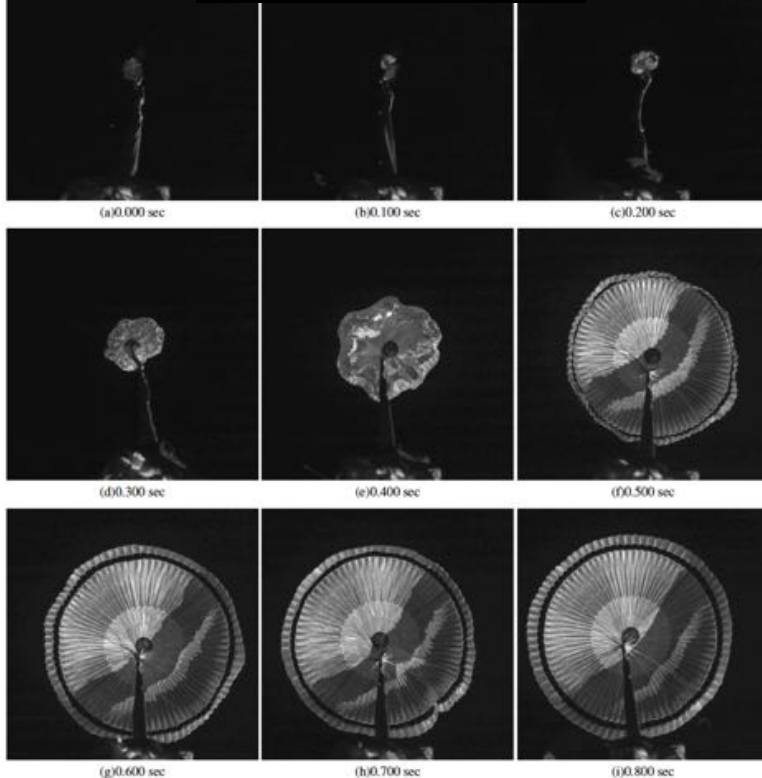


ASPIRE

Parachute Deployment and Inflation



Parachute Inflation Sequence



Mortar Fire
L+161 s
Alt: 42 km
 q_{∞} : 453 Pa
Mach: 1.77

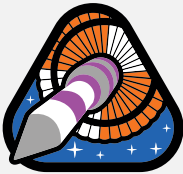
Line Stretch
MF + 0.96 s
 q_{∞} : 491 Pa
Mach: 1.79

Peak Load
MF +1.47 s
 q_{∞} : 500 Pa
Mach: 1.77

© 2017 Google
Data SIO, NOAA, U.S. Navy, NGA, GEBCO
Data LDEO, Columbia, NSF, NOAA
Image Landsat - Copernicus

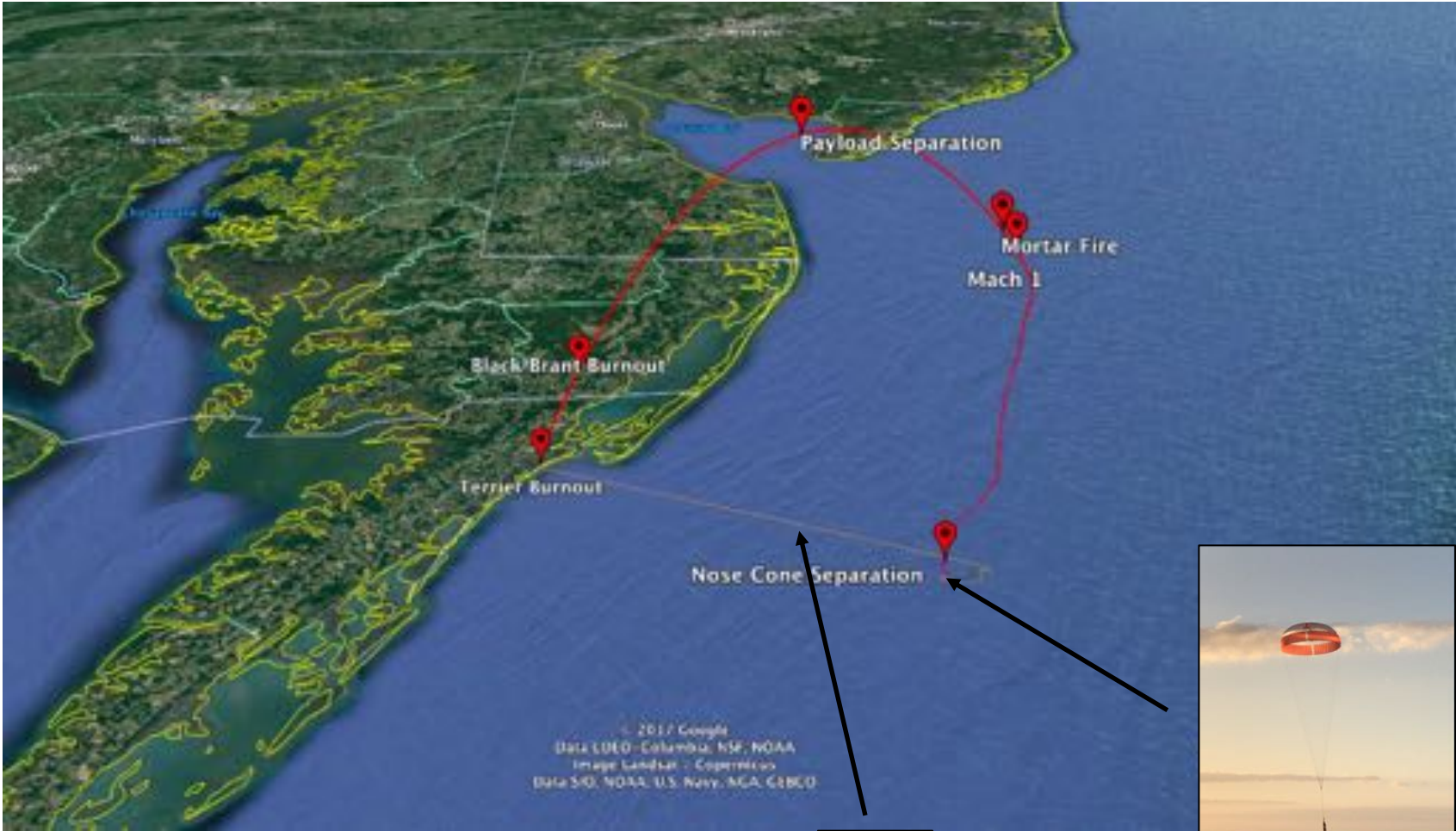
Google Earth

SR01 Flight Test

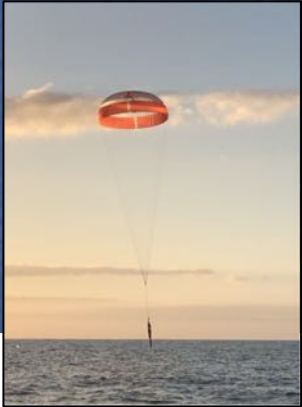


ASPIRE

Splashdown and Recovery

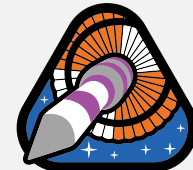


Range
55 km



Splashdown
L+ 34 min

SR01 Flight Test Summary

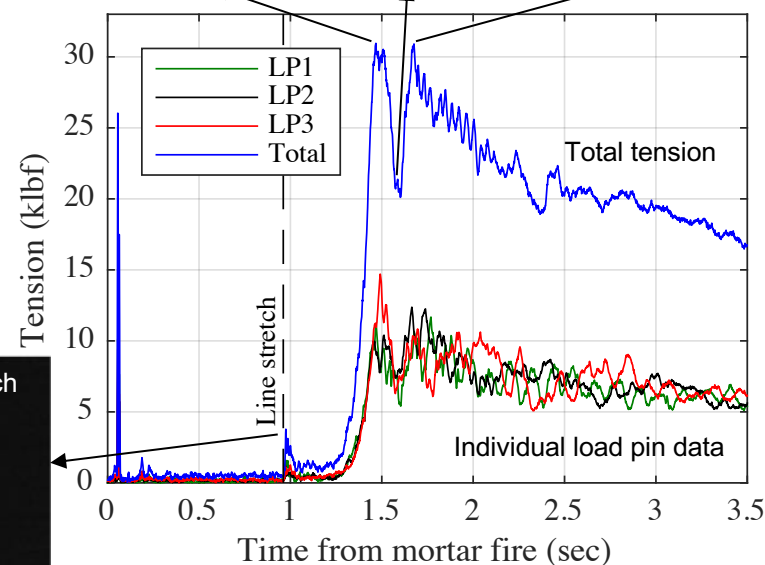
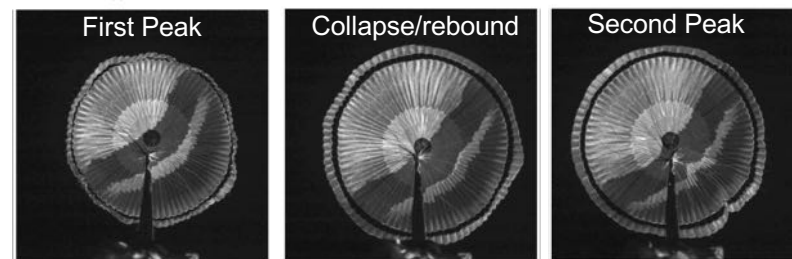


ASPIRE

| Event | Time from launch (sec) | Mach number | Dynamic pressure (Pa) | Wind-relative velocity (m/s) | Geodetic altitude (km) |
|--------------------|------------------------|-------------|-----------------------|------------------------------|------------------------|
| Payload Separation | 104.03 | 1.27 (1.2) | 87.15 (86.1) | 407.8 | 49.92 (49.9) |
| Apogee | 119.04 | 1.19 | 65.74 | 379.66 | 51 (50.9) |
| Mortar Fire | 161.41 | 1.77 (1.74) | 452.53 (438.4) | 560.29 | 42.4 |
| Peak Load | 162.88 | 1.77 (1.72) | 494.88 (473.0) | 560.94 | 41.8 |

() Pre-flight prediction

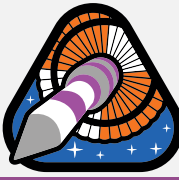
- Exceeded dynamic pressure at peak load by 4.6% (All the flight events were very close to pre-flight predictions)
- Load pins in the parachute assembly measure the tension (Parachute force = tension + payload mass x acceleration)
- Peak Aerodynamic Load = 32.4 k lbf = 144.07 kN (Pre-flight prediction 35 k lbf)
- Inflation load indicator $F_{peak} = k_p(2q_{\infty}S_p)$
Reconstructed k_p : 0.77 (pre-flight range: 0.76 - 0.98)
- Force trace shows oscillations of roughly 20Hz frequency (close to the parachute system frequency)



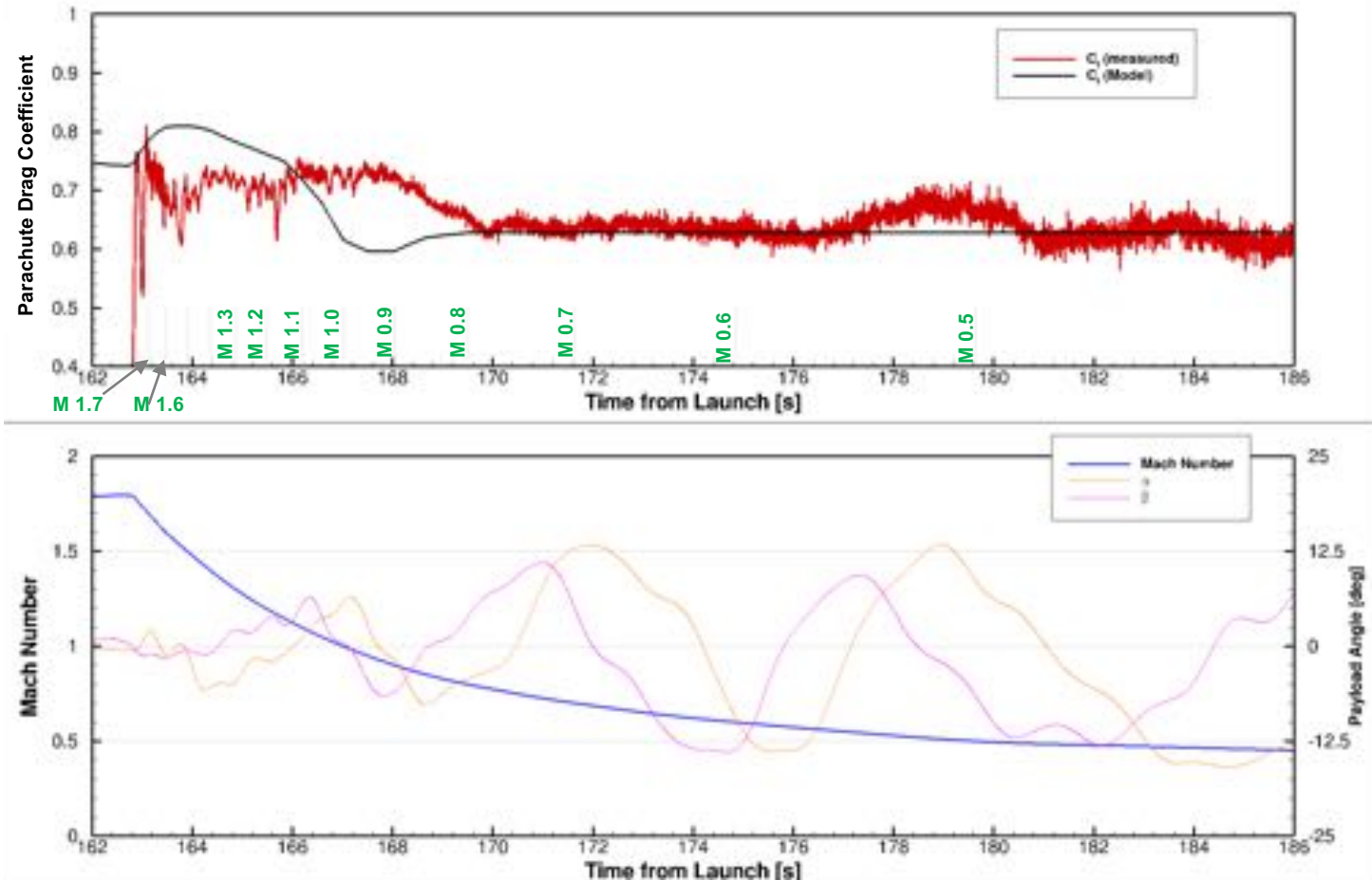
SR01 was successful.

- Validated Parachute test approach
- Met all test objectives.
- Yielded imagery and loads

Parachute Drag Performance

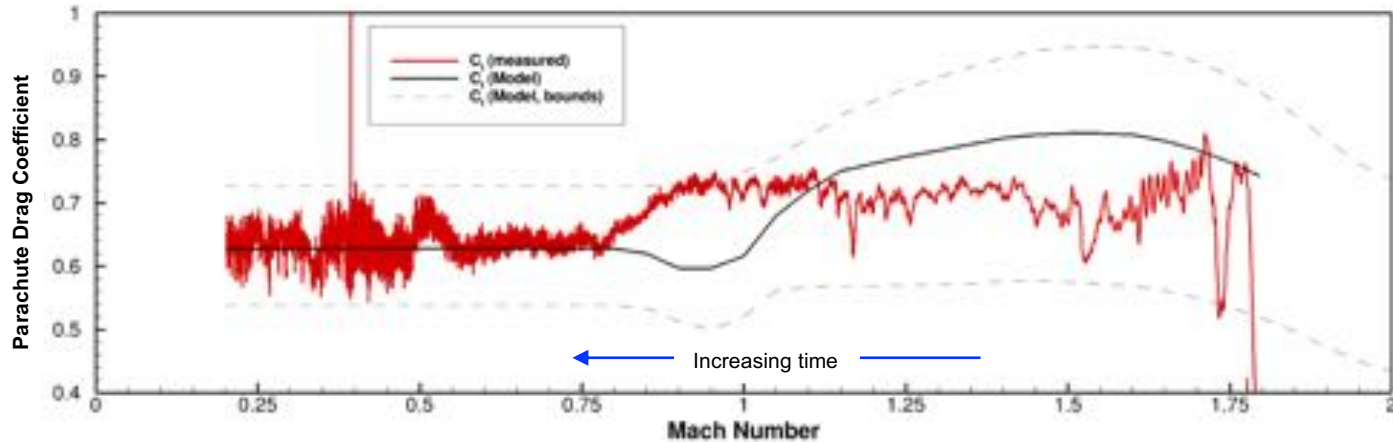


ASPIRE



- Good agreement between modeled and measured drag (coefficient) below M 0.75; over-prediction above 1.15 (Vehicle attitude and parachute pull vector fairly small during this period)
- Test data does not exhibit a transonic reduction in drag (ongoing work: *Is the transonic drag reduction related to the leading body geometry?*)

Parachute Drag Performance



- Image shows test data against pre-flight model along with the (upper and lower) bounds
- Except for a brief instant near Mach 0.85, the entire test data (roughly 30 min) is well within the bounds
- Pre-flight model, bounds, used in flight mechanics simulations (*next presentation*) are reasonable
- This was the first of several ASPIRE flight tests planned; flight test data did not justify need to change parachute drag model for the second flight test.
- Parachute drag performance during SR02 (March 2018) was very similar to SR01.

Conclusions



- ASPIRE project is testing supersonic parachutes at Mars relevant conditions
- Numerical simulations helped generate models for parachute inflation, deployment and loads (which in turn were used to target the flight test).
- First flight test (SR01) took place on 4th October 2017
- The parachute was successfully deployed at the target conditions; force data and imagery were obtained.
 - Mach Number 1.77
 - Altitude 42 km
- Pre-flight parachute drag model compares well to the flight test measurements.
 - Supersonic parachute drag was over-predicted by about 10%
 - Test data does not exhibit transonic drag reduction
 - Subsonic parachute drag was well-predicted
- Second flight test (SR02) took place in March 2018
- Third flight test (SR03) is scheduled for July 2018
- Ongoing analysis
 - 3D parachute shape reconstruction from stereo videogrammetry
 - Investigation of supersonic drag: CFD simulations at flight-like conditions & geometry
 - Static aerodynamic coefficients & parachute/payload dynamics